Figure S1: Biweekly time-series (x axis indicates numeric week starting in Jan 2018) for epidemiologically linked cases (y axis) in each of the 22 regions of Madagascar. Christmas 2018 (grey rectangle) often corresponds to a reduction in growth of the epidemic, presumably linked to reduced aggregation of individuals occurring during holidays. Approximate timing of the waves of vaccination in each region are shown as dashed vertical lines; the fraction of the population reached in each region in each of the three waves in shown in Table S1. This representation indicates that in some cases, the vaccination waves were unfortunately late relative to the timing of the outbreak (e.g., Androy).

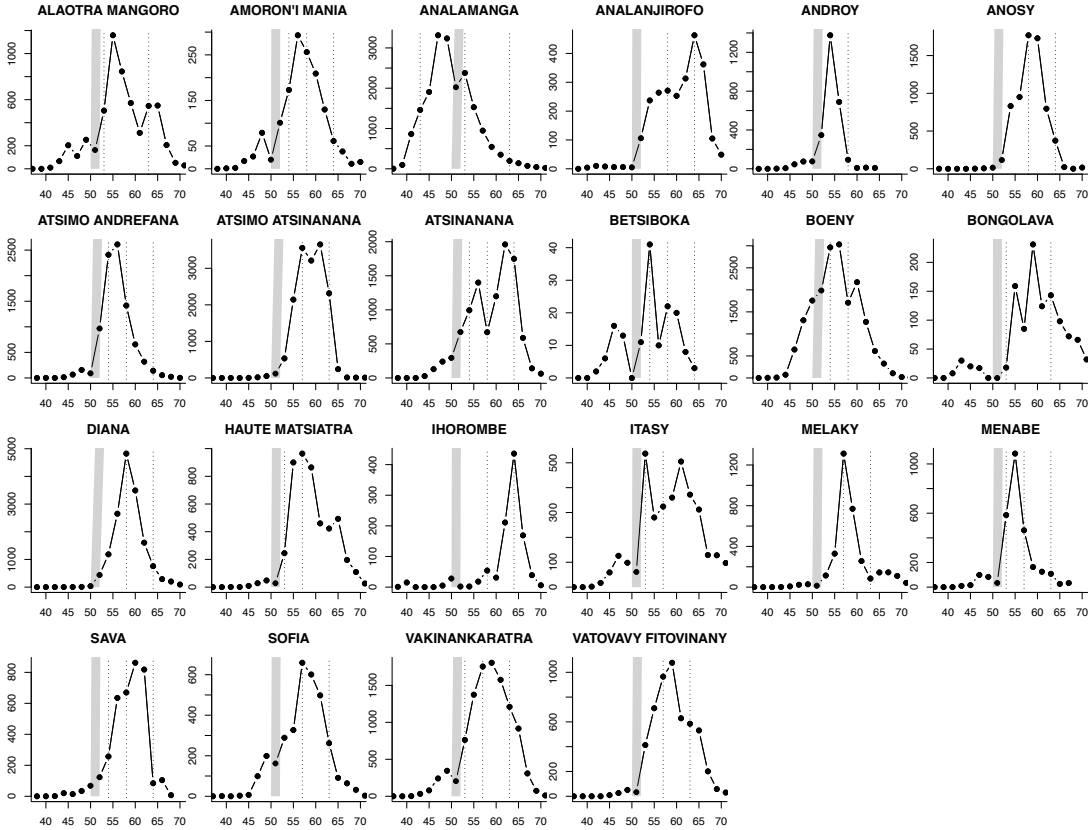

Figure S2: A) Measles age-specific seroprevalence by province in 2014-2015 based on residual febrile/rash samples. B) Total number of measles suspected cases by age in the 2018-19 outbreak by province.

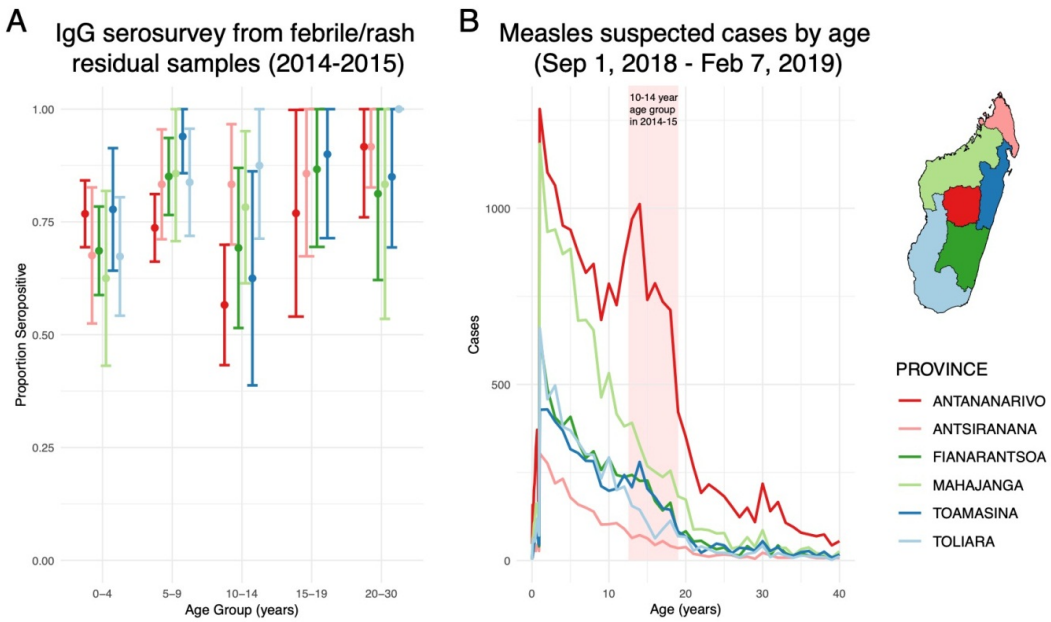

Figure S3: The age range of reported cases is relatively invariant over the course of the outbreak (x axis is time in weeks since the start of 2018, y axis is age in years, colour indicates the proportion of cases concentrated at each age over time, vertical black line indicates Christmas 2018). A fitted generalized additive model of age as function of week for each region (or province) revealed only very slight changes in age over the course the outbreak, associated with very small fractions of the variation explained (<1% across scenarios). Cases occur in individuals aged >10 years, the upper range targeted by vaccination (horizontal grey line).

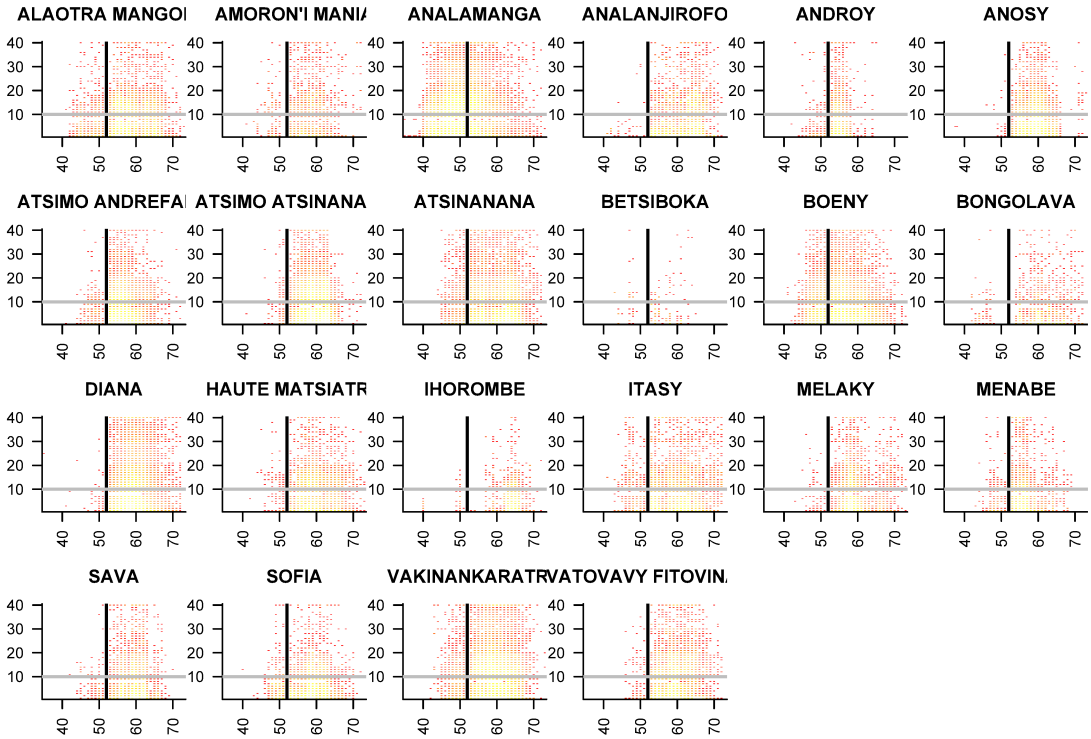

Table S1: **Expected coverage by region in each of the three waves of vaccination.** All districts within each of the regions of Madagascar were ultimately targeted (i.e., by April), with a known subset of districts targeted within each wave of vaccination. To understand the degree to which vaccination might have been concentrated early/late within each region, and in the absence of more fine scale information, we assumed that vaccination coverage reached the same fraction of the target population within each district. From this assumption, the fraction of each region reached within each wave can be captured by knowing the fraction of the population of that region that lives in the districts targeted in each wave (ignoring the nuance of age distributions, given all the other sources of uncertainty). We used estimates of the population size distribution across districts from worldpop.org.uk to obtain the proportion of each region targeted in each wave.

Region	Jan wave	Feb wave	Mar/April wave
ALAOTRA MANGORO	0.84	0	0.16
AMORON I MANIA	0.37	0.28	0.35
ANALAMANGA	0.90	0	0.10
ANALANJIROFO	0	0.51	0.49
ANDROY	0	1.00	0
ANOSY	0	0.40	0.60
ATSIMO ANDREFANA	0.11	0.78	0.12
ATSIMO ATSINANANA	0	0.94	0.06
ATSINANANA	0.40	0.30	0.30
BETSIBOKA	0.51	0.42	0.07
BOENY	0.50	0.50	0
BONGOLAVA	0.72	0	0.28
DIANA	0	0.85	0.15
HAUTE-MATSIATRA	0.16	0.84	0
IHOROMBE	0	0.65	0.35
ITASY	0.41	0.59	0
MELAKY	0	0.61	0.39
MENABE	0.20	0.67	0.13
SAVA	0.23	0.51	0.25
SOFIA	0	0.54	0.46
VATOVAVY FITOVINANY	0	0.72	0.28
VAKINANKARATRA	0.67	0.11	0.22

Supplementary text.

Many lines of evidence suggest the outbreak was driven by late age immunity gaps. An alternative possibility is that later aged suspected cases (Figure 2A) have another aetiology (e.g., rubella virus), a question requiring attention since a large fraction of suspected cases serologically tested for measles IgM (a short term marker of infection) were seronegative (46% out of n=3094 of the most recent data). However, rates of laboratory confirmation did not vary over age ($p>0.1$ for age as an explanatory variable of measles seropositivity using a generalized additive model) confirming that older aged susceptible individuals played a large role in the outbreak. Furthermore, the ages where infection is concentrated approximately map to the age groups identified by the earlier febrile/rash-based serological survey for measles susceptibility (Figure S2).